Submitted to Phys. Rev. Lett. E-Print astro-ph/9604093



# Highest Energy Cosmic Rays, Grand Unified Theories, and the Diffuse Gamma-Ray Background

Günter Sigl and Sangjin Lee
*Department of Astronomy & Astrophysics, Enrico Fermi Institute, The University of Chicago, Chicago, IL 60637-1433 and NASA/Fermilab Astrophysics Center, Fermi National Accelerator Laboratory, Batavia, IL 60510-0500*

Paolo Coppi
*Department of Astronomy, Yale University, New Haven, CT 06520-8101*

We explore scenarios where the highest energy cosmic rays (HECR) are produced by new particle physics near the grand unification scale. Using detailed numerical simulations of extragalactic cosmic and $\gamma$-ray propagation, we show the existence of a significant parameter space for which such scenarios are consistent with all observational constraints. An average fraction of $\simeq 10\%$ $\gamma$-rays in the total cosmic ray flux around 10 EeV ($10^{19}$ eV) would imply both a non-acceleration origin of HECR and a large scale extragalactic magnetic field $\lesssim 10^{-11}$ G. Proposed observatories for ultra-high energy cosmic rays should be able to test for this signature.

PACS numbers: 98.70.Sa, 98.70.Vc, 98.80.Cq, 95.30.Cq

The HECR events observed above 100 EeV [1,2] are difficult to explain within conventional models involving first order Fermi acceleration of charged particles at astrophysical shocks [3]. It is hard to accelerate protons and heavy nuclei up to such energies even in the most powerful astrophysical objects [4], like radio galaxies and active galactic nuclei. Also, nucleons above $\simeq 70$ EeV undergo photopion production on the cosmic microwave background (CMB), which is known as the Greisen-Zatsepin-Kuzmin (GZK) effect [5] and limits the distance to possible sources to less than $\simeq 100$ Mpc [6]. Heavy nuclei are photodisintegrated in the CMB within a few Mpc [7]. There are no obvious astronomical sources within $\simeq 100$ Mpc of the Earth.

A way around these difficulties is to suppose the HECR are created directly at energies comparable to or exceeding the observed ones rather than being accelerated from lower energies. In the current versions of such "top-down" (TD) scenarios, predominantly $\gamma$-rays and neutrinos are initially produced at ultra-high energies (UHEs) by the quantum mechanical decay of supermassive elementary "X" particles related to some grand unified theory (GUT). Such X particles could be released from topological defect relics of phase transitions which might have been caused by spontaneous breaking of GUT symmetries in the early universe [8]. TD models of this type are attractive because they predict injection spectra which are considerably harder than shock acceleration spectra and, unlike the GZK effect for nucleons, there is no threshold effect in the attenuation of UHE $\gamma$-rays which dominate the predicted flux.

There has been considerable discussion in the literature whether the $\gamma$-ray, nucleon, and neutrino fluxes predicted by TD scenarios are consistent with observational data and constraints at any energy [9–12]. The absolute flux levels predicted by TD models are in general extremely uncertain [13]. Accordingly, in this letter we treat the production rate of decaying X particles as a free parameter to be adjusted to match data and constraints. (We note that TD scenarios such as annihilation of magnetic monopole-antimonopole pairs [14] *can* yield HECR fluxes consistent with observations without violating bounds on monopole abundances.) Under this "optimal" assumption, we then use detailed numerical simulations of extragalactic cosmic and $\gamma$-ray propagation to show that TD models are still viable for an interesting range of parameters. We also explore a signature for TD mechanisms based on the isotropic component of the $\gamma$-ray flux below 100 EeV, particularly around 10 EeV. The exposure required to test this signature is significantly smaller than for measurements above 100 EeV (e.g., as proposed in Refs. [15] and [16]), as long as discrimination between $\gamma$-rays and charged cosmic rays (CRs) is possible at a level of a few percent. This is within the reach of proposed experiments [17].

*Top-Down Models.* The X particles released, say, in the annihilation or collapse of defects such as cosmic strings, monopoles, or domain walls could be gauge bosons, Higgs bosons, superheavy fermions, etc. depending on the specific GUT. Thses X particles would have a mass $m_X$ comparable to the symmetry breaking scale and would rapidly decay typically into a lepton and a quark of

roughly comparable energy. We take the primary lepton produced in a decay to be an electron with energy $m_X/2$. (Prior calculations have ignored this lepton which is not a good approximation given the lepton's energy.) The quark interacts strongly and hadronizes into nucleons ($N$s) and pions, the latter decaying in turn into $\gamma$-rays, electrons, and neutrinos. Given the X particle production rate, $dn_X/dt$, the effective injection spectrum of particle species $a$ ($a = \gamma, N, e^{\pm}, \nu$) via the hadronic channel can be written as $(dn_X/dt)(2/m_X)(dN_a/dx)$, where $x \equiv 2E/m_X$, and $dN_a/dx$ is the relevant fragmentation function. For the total hadronic fragmentation function $dN_h/dx$ we use solutions of the QCD evolution equations in modified leading logarithmic approximation which provide good fits to accelerator data at LEP energies [18]. We assume that about 3% of the total hadronic content consists of nucleons and the rest is produced as pions and distributed equally among the three charge states. The standard pion decay spectra then give the injection spectra of $\gamma$-rays, electrons, and neutrinos. The X particle injection rate is assumed to be spatially uniform and in the matter-dominated era can be parametrized as $dn_X/dt \propto t^{-4+p}$ [8], where $p$ depends on the specific defect scenario. In this letter we focus on the case $p = 1$ which is representative for a network of ordinary cosmic strings [19] and annihilation of monopole-antimonopole pairs [14].

*Numerical Simulations.* The $\gamma$-rays and electrons produced by X particle decay initiate electromagnetic (EM) cascades on low energy radiation fields such as the CMB. The high energy photons undergo electron-positron pair production (PP; $\gamma\gamma_b \to e^-e^+$), and at energies below $\sim 10^{14}$ eV they interact mainly with the universal infrared and optical (IR/O) background, while above $\sim 100$ EeV they interact mainly with the universal radio background (URB). In the Klein-Nishina regime, where the center of mass energy is large compared to the electron mass, one of the outgoing particles usually carries most of the initial energy. This "leading" electron (positron) in turn can transfer almost all of its energy to a background photon via inverse Compton scattering (ICS; $e\gamma_b \to e'\gamma$). EM cascades are driven by this cycle of PP and ICS. The energy degradation of the "leading" particle in this cycle is slow, whereas the total number of particles grows exponentially with time. This makes a standard Monte Carlo treatment difficult. We have therefore used an an implicit numerical scheme to solve the relevant kinetic equations. A detailed account of our transport equation approach is in Ref. [20]. We include all EM interactions that influence the $\gamma$-ray spectrum in the energy range $10^8\,\mathrm{eV} < E < 10^{25}\,\mathrm{eV}$, namely PP, ICS, triplet pair production (TPP; $e\gamma_b \to ee^-e^+$), and double pair production ($\gamma\gamma_b \to e^-e^+e^-e^+$). The relevant nucleon interactions implemented are pair production by protons ($p\gamma_b \to pe^-e^+$), photoproduction of single or multiple pions ($N\gamma_b \to N\ n\pi$, $n \geq 1$), and neutron decay. Production of secondary $\gamma$-rays, electrons, and neutrinos by pion decay is also included. We assume a flat universe with no cosmological constant, and a Hubble constant of $H_0 = 75\,\mathrm{km\ sec^{-1}Mpc^{-1}}$ throughout. An important difference with respect to past work is that we follow *all* produced particles, whereas the often-used continuous energy loss (CEL) approximation (e.g., [16]) follows only the leading cascade particles. We find that the CEL approximation can significantly underestimate the cascade flux at lower energies.

Similar studies using somewhat different numerical techniques have been performed for the case of discrete sources injecting $\gamma$-rays and nucleons monoenergetically [11] and more recently for fragmentation functions $\propto x^{-1.5}(1-x)^2$ and spatially uniform injection [12].

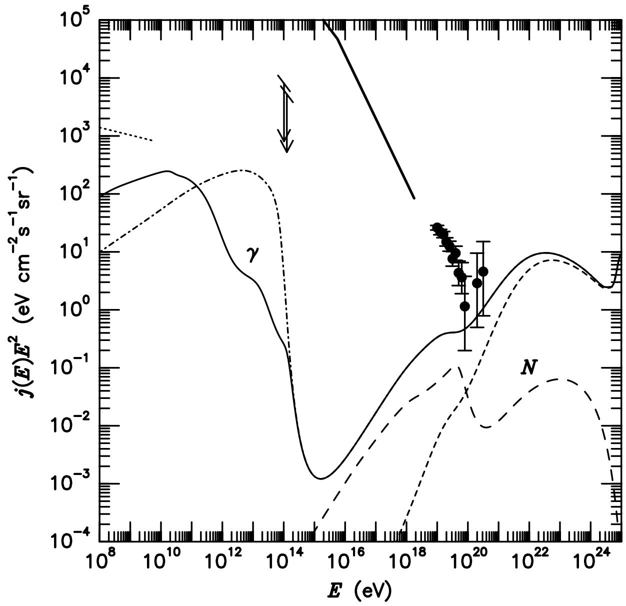


FIG. 1. Predictions for the differential fluxes of $\gamma$-rays (solid line) and nucleons (long dashed line) by a TD model characterized by $p = 1$, $m_X = 2 \times 10^{16}\,\mathrm{GeV}$, for no EGMF. The dashed line shows the $\gamma$-ray flux predicted by the CEL approximation. The dash-dotted line shows the result when there is no IR/O background. Also shown are the combined data from the Fly's Eye [1] and the AGASA [2] experiments above 10 EeV (dots with error bars), piecewise power law fits to the observed charged CR flux (thick solid line) and experimental upper limits on the $\gamma$-ray flux at $1 - 10\,\mathrm{GeV}$ from EGRET data [22] (dotted line on left margin). The arrows indicate limits on the $\gamma$-ray flux from Ref. [23].

*Results.* Fig. 1 shows the results for the $\gamma$-ray and nucleon fluxes from a typical TD scenario, assuming no EGMF, along with current observational constraints on the $\gamma$-ray flux. The spectrum was normalized in the best possible way to allow for an explanation of the observed HECR events, assuming their consistency with a nucleon or $\gamma$-ray primary (although a $\gamma$-ray primary is somewhat disfavored [21]). The flux below $\lesssim 20$ EeV

is presumably due to conventional acceleration and was not fit. The shapes of our spectra are similar to those of Ref. [12]. However, they normalize their spectra to match the observed differential flux at 300 EeV, which then leads to an overproduction of the integral flux at higher energies. We remark that above 100 EeV, the fits shown in Figs. 1 and 2 have likelihood significances above 50% (see Ref. [15] for details) and are consistent with the integral flux above 300 EeV esitmated in Refs. [1,2]. Since the energy injected at high redshifts is recycled by cascading to lower energies, TD models are significantly constrained [9,10] by current limits on the diffuse $\gamma$-ray background at $1-10$ GeV [22]. Note that the IR/O background strongly depletes the background in the range $10^{11}-10^{14}$ eV, recycling it to energies below 10 GeV (see Fig. 1). The predicted background is *not* very sensitive to the specific IR/O background model, however [24]. Constraints from limits on CMB distortions and light element abundances from $^4$He-photodisintegration are comparable to the bound from the directly observed $\gamma$-rays [10]. The scenario in Fig. 1 obeys all current constraints within the normalization ambiguities and is therefore quite viable.

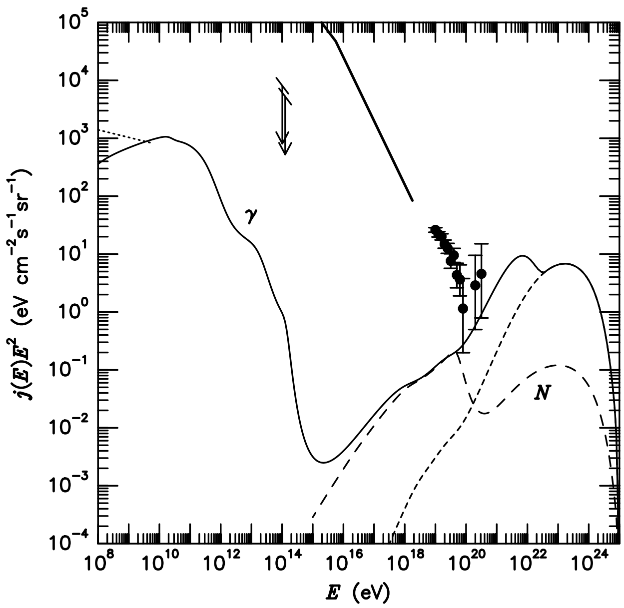


FIG. 2. Same as Fig. 1, but for an EGMF of $10^{-9}$ G.

Fig. 2 shows results for the same TD scenario as in Fig. 1, but for a high EGMF $\sim 10^{-9}$ G (near the current upper limit [26]). In this case, rapid synchrotron cooling of the initial cascade pairs quickly transfers energy out of the UHE range. The UHE $\gamma-$ray flux then depends mainly on the absorption length due to pair production and is typically much lower [16,25]. (Note, though, that for $m_X \gtrsim 10^{25}$ eV, the synchrotron radiation from these pairs can be above 100 EeV, and the UHE flux is then not as low as one might expect.) To match the HECR flux, we must inject more X particles, which leads to a factor $\sim 5$ increase in the $\gamma-$ray background expected below 10 GeV. For a high EGMF, the constraints from the flux limits below 10 GeV are much more severe and in general, TD scenarios in a high EGMF are only marginally allowed.

The energy loss and absorption lengths for UHE nucleons and photons are short ($\lesssim 100$ Mpc). Thus, their predicted UHE fluxes are independent of cosmological evolution. The $\gamma-$ray flux below $\simeq 10^{11}$ eV, however, scales as the total X particle energy release integrated over all redshifts and increases with decreasing $p$ [10]. For $m_X = 2\times10^{16}$ GeV, scenarios with $p<1$ are therefore ruled out (see Figs. 1 and 2), whereas constant comoving injection rates ($p=2$) are well within the limits. As the EM flux above $\simeq 10^{22}$ eV is efficiently recycled to lower energies, the constraint on $p$ is insensitive to $m_X$ for low EGMF. This in contrast to earlier CEL-based analytical estimates [9,10].

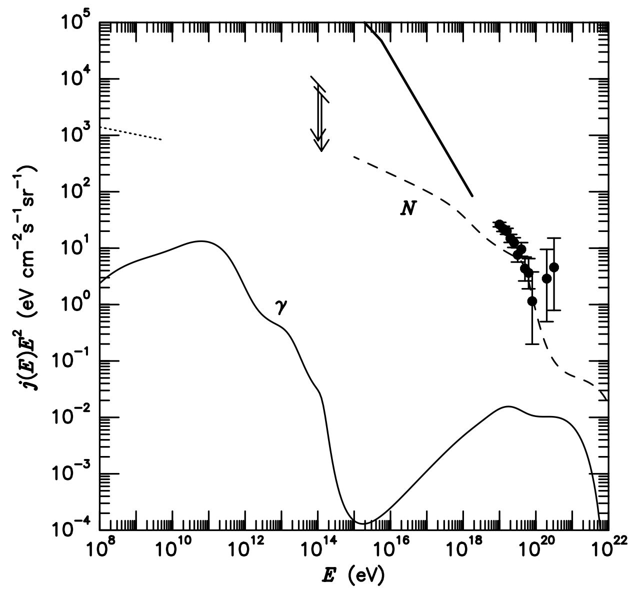


FIG. 3. Predictions for the differential fluxes of $\gamma$-rays (solid line) and nucleons above $10^{15}$ eV (long dashed line) by a uniform, constant comoving density of shock acceleration sources up to a redshift of 4, injecting protons with a spectrum $\propto E^{-2.3}$ up to $10^{22}$ eV, for a vanishing EGMF.

We now turn to signatures of TD models at UHEs. For low EGMF (e.g., Fig. 1), the full cascade calculation predicts $\gamma$-ray fluxes below 100 EeV an order of magnitude higher than those obtained using the CEL approximation. Again, this shows the importance of non-leading particles in the development of unsaturated EM cascades at energies below $\sim 10^{22}$ eV. Our numerical simulations give a $\gamma$/CR flux ratio at 10 EeV of $\simeq 0.1$. The experimental exposure required to detect a $\gamma$-ray flux at that level is $\simeq 4\times10^{19}$ cm$^2$ sec sr, about a factor 10 smaller than the current total experimental exposure. These

exposures are well within reach of the proposed Pierre Auger Cosmic Ray Observatories [17], which may be able to detect a neutral CR component down to a level of 1% of the total flux. In contrast, if the EGMF exceeds $\sim 10^{-11}$ G, then UHE cascading is inhibited, resulting in a lower UHE $\gamma$-ray spectrum. In the $10^{-9}$ G scenario of Fig. 2, the $\gamma$/CR flux ratio at 10 EeV is $\simeq 4 \times 10^{-3}$, significantly lower than for no EGMF.

Another not well known factor affecting UHE $\gamma$-ray propagation is the URB for which we used the spectrum suggested in Ref. [27]. A higher overall URB amplitude correspondingly reduces the $\gamma$-ray flux, but without significantly changing its spectral shape. Thus, as long as $\gamma$-rays dominate nucleons in the TD component above $\simeq 100$ EeV and the total flux is normalized to the HECR events, predictions for the $\gamma$/CR flux ratio below $\simeq 100$ EeV are essentially independent of the URB amplitude and the hadronic fraction at injection. An URB cutoff frequency lower than 2 MHz (the value we took) affects this ratio in a less trivial way with a tendency to smaller $\gamma$/CR values.

Fig. 3 shows spectra resulting from a typical non-TD scenario, in this case a uniform distribution of shock acceleration sources. Such a scenario gives a UHE CR spectrum with a GZK cutoff and $\gamma$-rays are only produced as secondaries. Our treatment of multiple pion production by nucleons leads to secondary $\gamma$-ray fluxes somewhat higher than in Refs. [11,28]. The key point is that the (isotropic) $\gamma$/CR flux ratio is $\lesssim 10^{-3}$ at 10 EeV, much smaller than predicted by TD models in a small EGMF. Ratios as high as 10% can only be reached in the direction of powerful nearby acceleration sources. The secondary $\gamma$-ray flux generally decreases still further with decreasing maximum injection energy and increasing EGMF [25].

In summary, some TD-type scenarios for the HECR origin are still unconstrained by current data and bounds on $\gamma$-ray and UHE CR fluxes. For example, if the mean EGMF is $\lesssim 10^{-9}$ G, spatially uniform annihilation of magnetic monopoles and antimonopoles is still a viable model for GUT scales up to $10^{16}$ GeV. A solid angle averaged $\gamma$/CR flux ratio $\simeq 10\%$ at $\sim 10$ EeV would be hard to explain by a conventional acceleration origin of HECRs, and assuming the TD picture holds, would place an independent upper limit of $\simeq 10^{-11}$ G on the poorly known EGMF on scales of a few to tens of Mpc. Absence of a high $\gamma$/CR flux at this level either rules out a TD origin for HECRs or implies an EGMF strength $\gtrsim 10^{-11}$ G. A test of this signature should be possible with currently proposed experiments. TD models also predict significant neutrino fluxes. Implications of this will be considered in a separate publication [29].

We thank W. Ochs, D. N. Schramm, J. W. Cronin, Chris Hill, and F. A. Aharonian for stimulating discussions and Shigeru Yoshida for comments. This work was supported by DOE, NSF and NASA at the University of Chicago, by the DOE and by NASA through grant NAG5-2788 at Fermilab, and by the Alexander-von-Humboldt Foundation. SL acknowledges the support of the POSCO Scholarship Foundation in Korea.

---

[1] D. J. Bird *et al.*, Phys. Rev. Lett. **71**, 3401 (1993); Astrophys. J. **424**, 491 (1994); *ibid.* **441**, 144 (1995).

[2] N. Hayashida *et al.*, Phys. Rev. Lett. **73**, 3491 (1994); S. Yoshida *et al.*, Astropart. Phys. **3**, 105 (1995).

[3] for a review see, e.g., R. Blandford and D. Eichler, Phys. Rep. **154**, 1 (1987).

[4] A. M. Hillas, Ann. Rev. Astron. Astrophys. **22**, 425 (1984).

[5] K. Greisen, Phys. Rev. Lett. **16**, 748 (1966); G. T. Zatsepin and V. A. Kuzmin, Pisma Zh. Eksp. Teor. Fiz. **4**, 114 (1966) [JETP. Lett. **4**, 78 (1966)].

[6] G. Sigl, D. N. Schramm, and P. Bhattacharjee, Astropart. Phys. **2**, 401 (1994).

[7] J. L. Puget, F. W. Stecker, and J. H. Bredekamp, Astrophys. J. **205**, 638 (1976).

[8] P. Bhattarcharjee, C. T. Hill, and D. N. Schramm, Phys. Rev. Lett. **69**, 567 (1992).

[9] X. Chi *et al.*, Astropart. Phys. **1**, 129 (1993); *ibid.* **1**, 239 (1993).

[10] G. Sigl, K. Jedamzik, D. N. Schramm, and V. Berezinsky, Phys. Rev. D **52**, 6682 (1995).

[11] R. J. Protheroe and P. A. Johnson, Astropart. Phys. **4**, 253 (1996).

[12] R. J. Protheroe and T. Stanev, report ADP-AT-96-6, astro-ph/9605036, submitted to Phys. Rev. Lett.

[13] A. J. Gill and T. W. B. Kibble, Phys. Rev. D **50**, 3660 (1994).

[14] P. Bhattarcharjee and G. Sigl, Phys. Rev. D **51**, 4079 (1995).

[15] G. Sigl, S. Lee, D. N. Schramm, and P. Bhattacharjee, Science **270**, 1977 (1995).

[16] F. A. Aharonian, P. Bhattacharjee, and D. N. Schramm, Phys. Rev. D **46**, 4188 (1992).

[17] M. Boratav *et al.*, eds., Nucl. Phys. B (Proc. Suppl.) **28B** (1992).

[18] Yu. L. Dokshitzer, V. A. Khoze, A. H. Müller, and S. I. Troyan, *Basics of Perturbative QCD* (Editions Frontieres, Singapore, 1991).

[19] P. Bhattacharjee and N. C. Rana, Phys. Lett. B **246**, 365 (1990).

[20] S. Lee, report FERMILAB-Pub-96/066-A, astro-ph/9604098, submitted to Phys. Rev. D.

[21] F. Halzen, R. A. Vazquez, T. Stanev, and H. P. Vankov, Astropart. Phys. **3**, 151 (1995).

[22] A. Chen, J. Dwyer, and P. Kaaret, Astrophys. J. **463**, 169 (1996); C. E. Fichtel, *Proc. 3rd Compton Observatory Symposium*, Astron. Astrophys. Suppl., in press.

[23] A. Karle *et al.*, Phys. Lett. B **347**, 161 (1995).

[24] P. Coppi and F. Aharonian, submitted to Astrophys. J. Lett.

[25] S. Lee, A. V. Olinto, and G. Sigl, Astrophys. J. **455**, L21

(1995).
[26] P. P. Kronberg, Rep. Prog. Phys. **57**, 325 (1994).
[27] T. A. Clark, L. W. Brown, and J. K. Alexander, Nature **228**, 847 (1970).
[28] S. Yoshida and M. Teshima, Prog. Theor. Phys. **89**, 833 (1993).
[29] G. Sigl, S. Lee, and P. Coppi, in preparation.